Physics and Chemistry of the Earth xxx (xxxx) xxx–xxx

Contents lists available at ScienceDirect

Physics and Chemistry of the Earth

journal homepage: www.elsevier.com/locate/pce

Relating the dynamics of climatological and hydrological droughts in semiarid Botswana

Jimmy Byakatonda[a,c,*], B.P. Parida[a], Piet K. Kenabatho[b]

[a] Department of Civil Engineering, P/Bag, 0061, University of Botswana, Gaborone, Botswana
[b] Department of Environmental Science, P/Bag, 00704, University of Botswana, Gaborone, Botswana
[c] Department of Biosystems Engineering, Gulu University, P.O.Box 166, Gulu, Uganda

ARTICLE INFO

Keywords:
Nonlinear autoregressive with exogenous input neural network
Drought dynamics
Drought severity
Hurst coefficient
Standardized flow index
Standardized precipitation evapotranspiration index

ABSTRACT

Dynamics of droughts have been an associated feature of climate variability particularly in semiarid regions which impact on the response of hydrological systems. This study attempts to determine drought timescale that is suitable for monitoring the effects of drought on hydrological systems which can then be used to assess the long term persistence or reversion and forecasts of the dynamics. Based on this, climatological and hydrological drought indices characterized by Standardized precipitation evapotranspiration index (SPEI) and Standardized flow index (SFI) respectively have been determined using monthly rainfall, temperature and flow data from two major river systems. The association between climatological and hydrological droughts in Botswana has been investigated using these river systems namely: Okavango that is predominantly a storage type and Limpopo which is non-storage for a period of 1975–2014. Dynamics of climatological and hydrological droughts are showing trends towards drying conditions at both river systems. It was also observed that hydrological droughts lag climatological droughts by 7 months in Limpopo and 6 months in Okavango river systems respectively. Analyses of the association between climatic and flow indices indicate that the degree of association becomes stronger with increasing timescale at the Okavango river system. However in the Limpopo river system, it was observed that high timescales of 18- and 24-months were not useful in drought monitoring. 15-months timescale was identified to best monitor drought dynamics at both locations. Therefore SPEIs and SFIs computed at 15-months timescale have been used to assess the variability and long term persistence in drought dynamics through rescaled range analysis (R/S). H-coefficients of 0.06 and 0.08 resulted for Limpopo and Okavango respectively. These H-coefficients being significantly less than 0.5 is an indication of high variability and suggests a change in dynamics from the existing conditions in these river systems. To forecast possible changes, the nonlinear autoregressive with exogenous input (NARX) artificial neural network model has been used. Results from this model agree with those of the R/S and projects generally dry conditions for the next 40 months. Results from this study are helpful not only in choosing a proper timescale but also in evaluating the futuristic drought dynamics necessary for water resources planning and management.

1. Introduction

Drought is a form of hydrological extreme that is wide spread in temporal and spatial extent and is often referred to as 'creeping disaster' (Kundzewicz and Kaczmarek, 2000; Mishra and Singh, 2010; Van Loon, 2013). Impacts from droughts are likely to increase with the current rise in global temperature and reduction in precipitation (Dai, 2013, 2011; Solomon, 2007; Wada et al., 2011). Drought is not region specific, however most severe impacts of drought on population are seen to occur in arid and semiarid areas where available water resources are scarce even under normal conditions and the dwellers have limited adaptability options (De Stefano et al., 2012; Masih et al., 2014; Van Loon, 2013). This calls for studies on drought characteristics which will help in formulation of effective management strategies specific to these areas. Droughts have various definitions and classifications according to Wilhite (2000) and Sheffield et al. (2012). For purposes of this study, we shall confine ourselves to two common classifications viz: climatological and hydrological droughts. Climatological drought is defined as below normal precipitation coupled with increase in potential evapotranspiration covering large spatial extents for prolonged time periods (Rimkus et al., 2013; Van Loon, 2013; Van Loon and Laaha, 2015). While hydrological drought on the other hand is associated with below

* Corresponding author. Department of Civil Engineering, P/Bag, 0061, University of Botswana, Gaborone, Botswana.
E-mail address: byakatondaj@hotmail.com (J. Byakatonda).

https://doi.org/10.1016/j.pce.2018.02.004
Received 1 March 2017; Received in revised form 22 January 2018; Accepted 7 February 2018

average surface water flow for prolonged periods (Feyen and Dankers, 2009; Mishra et al., 2015; Smakhtin and Hughes, 2004). Hydrological droughts depend on a number of processes including the atmosphere and a host of other factors in the terrestrial part of the hydrological cycle that govern moisture transport (Mishra and Singh, 2010; Rimkus et al., 2013; Van Loon, 2013). The atmospheric processes that govern both climatological and hydrological droughts are believed to be linked to climate variability and change (Jung et al., 2010; Lorenzo-Lacruz et al., 2010; Van Loon, 2013). Response of hydrological systems are closely associated with climatic conditions in that decrease in precipitation with rising temperatures, increases potential evapotranspiration which leads to depletion of water and moisture storage (Lorenzo-Lacruz et al., 2010; Van Loon, 2013; Vicente-Serrano and López-Moreno, 2005). All these interactions between climatic and hydrological process are a function of a timescale. Since the hydrological systems respond at varying timescales, it calls for determination of that particular timescale at which a high degree of association between climatic and hydrological conditions exist to facilitate proper drought management. Semiarid regions have been known to generally experience high climate variability resulting in varying drought severity and impacts (Bazza, 2002; Wilhite et al., 2007). In view of this, better understanding of drought severity needs to be represented through drought indices which are proxies of drought impacts in a broader scale (Hayes et al., 2011; Rimkus et al., 2013; Svoboda et al., 2001). Both climatic and hydrological indices are proposed to be determined at various timescales to characterize drought dynamics (Lorenzo-Lacruz et al., 2010; Nalbantis and Tsakiris, 2009). The Standardized precipitation evapotranspiration index (SPEI) which incorporates both precipitation and temperature (Svoboda et al., 2016; Vicente-Serrano et al., 2010) to determine drought severity is proposed for use in explaining the dynamics of climatic drought under variable climate. Similarly, Standardized flow index (SFI) which is analogous to SPEI and standardized precipitation index (SPI) in their multiscalar nature has been proposed to be used to quantify the hydrological droughts (Byakatonda et al., 2016; Lorenzo-Lacruz et al., 2010; Nalbantis and Tsakiris, 2009; Svoboda et al., 2016; Trambauer et al., 2014). It is in this context that it may be necessary to determine the commonality in timescale for both the SPEI and SFI such that a general procedure can be established to determine such indices across the region covering various watersheds. However in recent times, it has also been observed that droughts often extend over longer timescales sometimes over the years with continued dry spells into the next hydrological year hence impacting on stream flow and over-the-year reservoir storage. This has been attributed to increased incidences of climate variability under global warming scenarios in semiarid locations (Dai, 2013; Huang et al., 2016; Masih et al., 2014). It hence becomes imperative to investigate variability and long term persistence or possible reversion in the drought dynamics. To achieve this, the study proposes the use of rescaled range analysis (R/S) with its associated Hurst coefficient to investigate variability in the dynamics at an identified timescale (Hurst, 1951; Koutsoyiannis, 2003). Additionally for the benefit of operational hydrologists and water managers, it may be necessary to develop a likely futuristic scenario over a limited period such that necessary drought management strategies if required could be developed. Drought being complex and nonlinear in nature, use of artificial intelligence oriented models such as artificial neural networks (ANN) have been proposed to be utilized in development of futuristic drought severity dynamics. A Nonlinear autoregressive with exogenous input (NARX) neural network model has been selected for use in this study to develop the likely scenarios across the river systems. This model has been successfully applied in complex hydrological time series simulations and proven to outperform other network configurations (Byakatonda et al., 2018a, 2018b, 2016; Chang et al., 2014; Menezes and Barreto, 2008). Hence this study attempts to determine dynamics of climatic and hydrological droughts at timescales of 3-, 6-, 12-, 18- and 24-months. The study further determines the drought timescale that is suitable for assessing the effects of climatic droughts on hydrological systems at the same time evaluates variability in the dynamics at the identified timescale. Climatic drought indices are also simulated over a medium time period of 60 months.

2. Materials and methods

2.1. Study area

Botswana which is located in the mid-latitudes lies between 16° S and 29° S, it is classified as arid to semiarid (FAO, 2001). The annual rainfall ranges from 300 mm in the southwest to 600 mm in the northeast with rain onset in November and ceding in March (Byakatonda et al., 2018b). It is reported that about 90% of the rainfall is received during the summer months of November, December and January (GOB-MMEWR, 2006). Botswana is selected as a study area due to its semiarid location. The study area has been reported to be experiencing low rainfall with increasing temperatures in the recent past (Batisani, 2012; Kenabatho et al., 2012; Parida and Moalafhi, 2008). Besides, precipitation is the main source of fresh water supply in Botswana with Limpopo river system being a host to most dams that supply majority of the water both for domestic and industrial use (GOB-MEWT, 2012). The main challenge Botswana faces in development of surface water storage are the recurrent droughts and high rates of evaporation which range from 1800 to 2100 mm/yr, exceeding the annual rainfall (Byakatonda et al., 2016). This is mainly as a result of high temperatures experienced during the summer rain season as shown in Figs. 2a and 3a. The water resources in the study area are mainly confined in four river systems viz: Okavango, Makgadikgad, Limpopo and Orange (GOB-MMEWR, 2006). The main rivers in Botswana are transboundary making water resources development a multi stakeholder involving process. The Okavango and Limpopo which are transboundary have more perennial water sources on which Botswana depends. Most of the inland water sources drain to the Limpopo river system which is used for water supply. This study used Limpopo and Okavango river systems as study sites (Fig. 1).

2.2. Datasets

2.2.1. Meteorological data

Climatic data comprising of monthly rainfall, maximum and minimum temperature were obtained from the Department of Meteorological Services (DMS) of Botswana for a period 1975–2014. The data is from 6 synoptic stations, 3 from each of the river systems as shown in Fig. 1. Number of earlier studies in the region have reported a shift in the climatic regime since 1980/81 (Parida and Moalafhi, 2008). The shift may be attributed to inhomogeneity in the climatic time series. For this reason, homogeneity tests were carried out on the data from the 6 synoptic stations used in this study. The homogeneity testing techniques applied include the standard normal homogeneity test (SNHT) (Alexandersson, 1986; Alexandersson and Moberg, 1997), Pettit test (Pettit, 1979) and the Buishand test (Buishand, 1982).

2.2.2. Hydrological data

The hydrological data was provided by the Department of Water Affairs of Botswana (DWA). The data consisted of monthly discharge recorded at Mohembo on River Okavango for a period from 1975 to 2014. The second gauging station was recorded at Buffel drift on River Limpopo with data spanning from 1997 to 2014. These stations were selected due to availability of consistent data with less than 10% missing values.

2.2.2.1. Okavango river system. The main river that supplies this system is River Okavango which enters Botswana from Angola at Mohembo (Fig. 1) and ends up as delta. The river system has been classified as a Ramsar site and therefore has restrictions on the extent of water

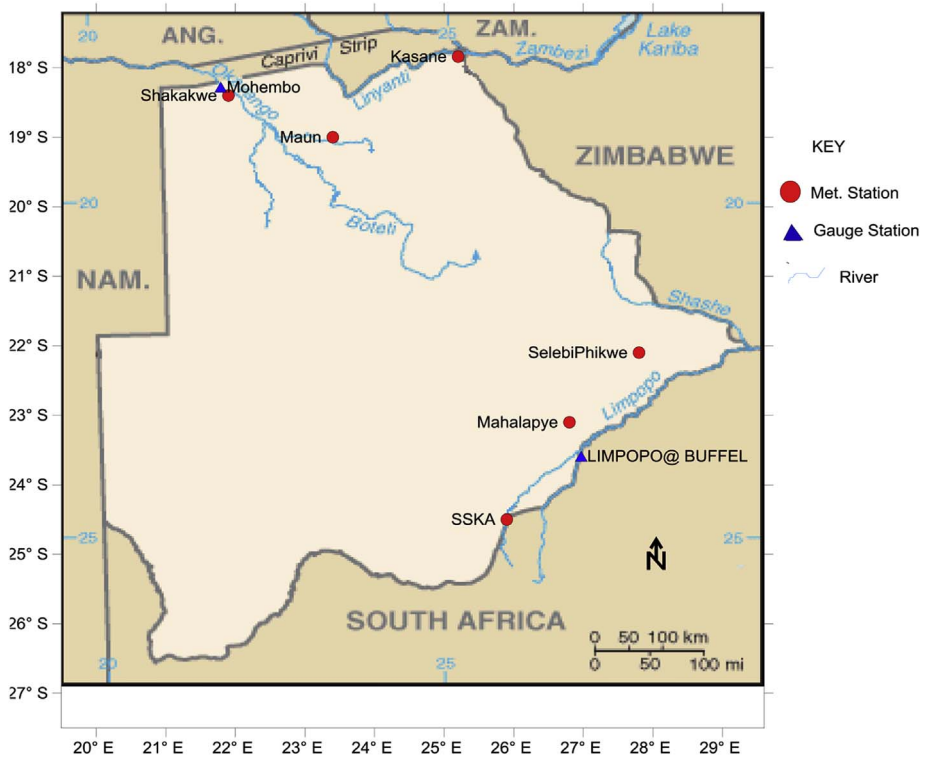

Fig. 1. Location of synoptic weather and river gauging stations in the study area.

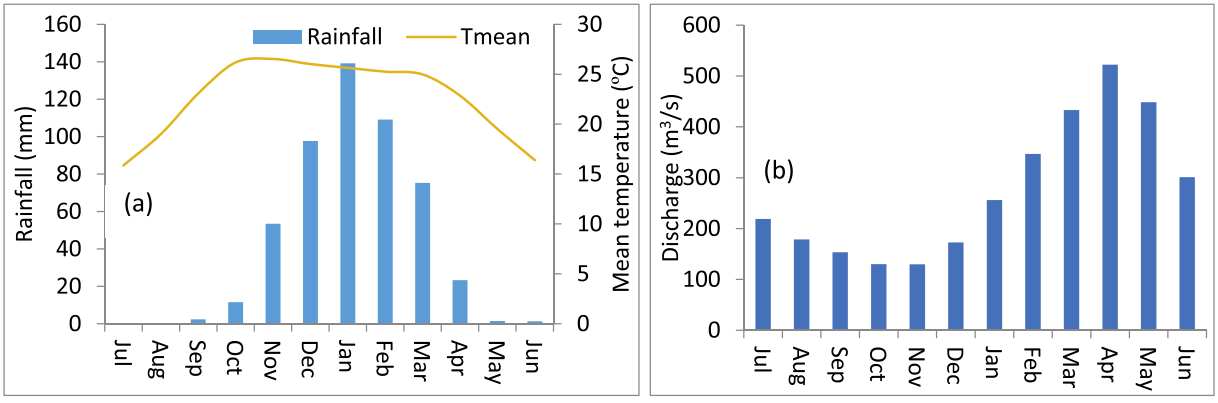

Tmean= mean temperature

Fig. 2. Monthly climatic and flow data in the Okavango river system (a) Areal rainfall and mean temperature (b) River Okavango discharge recorded at Mohembo.

resources development and abstractions (Byakatonda et al., 2016). This system mainly meets local water demand of the Panhandle with the rest of the resource reserved for ecological functions. It can be considered as a natural storage type river system where only losses are through evaporation and seepage. Majority of the rainfall over the Okavango river system occurs in the summer months from November to March as shown in Fig. 2a. At the same time temperature reaches its peak during the rain season as also shown in Fig. 2a implying that a high percentage of the available moisture is lost during this time period due to increased evaporative demand. Time series of monthly discharge shown in Fig. 2b indicate that flow starts to increase steadly from January reaching the peak in April and receding in May. It is evident that the peak flow almost occurs at the cessation of rains in the Okavango river system. For this reason it may be necessary to study the drought dynamics by investigating the hydrological response towards climatic droughts. This will enable establishment of a time lag and drought timescale necessary for monitoring over this river system which this study attempts to investigate.

2.2.2.2. Limpopo river system (Botswana sub-system). Majority of seasonal and permanent inland streams drain into the Limpopo river system including Notwane, Metsemotlhaba, Mahalapswe, Shashe, Tati, Ntshe, Ramokgwebana, Taupye, Bonwapitse, Thune and Lotsane (GOB-MMEWR, 2006). Most of these streams are heavily regulated with surface dams managed by Ministry of Minerals Energy and Water resources (MMEWR) for domestic, industrial supply and irrigation. These river sub systems have no clear topographical divide as they are characterized by a flat terrain (FAO, 2001). The river system derives its flows during the wet months and low flows are generally experienced for the rest of the year. It can be classified as a non-storage type of river system (except storage in artificial storage structures). As the case for the Okavango, the Limpopo river system also experiences the peak rain season in the months of December and January as shown in Fig. 3a. Discharge plot in Fig. 3b shows that peak flow occurs in March equally

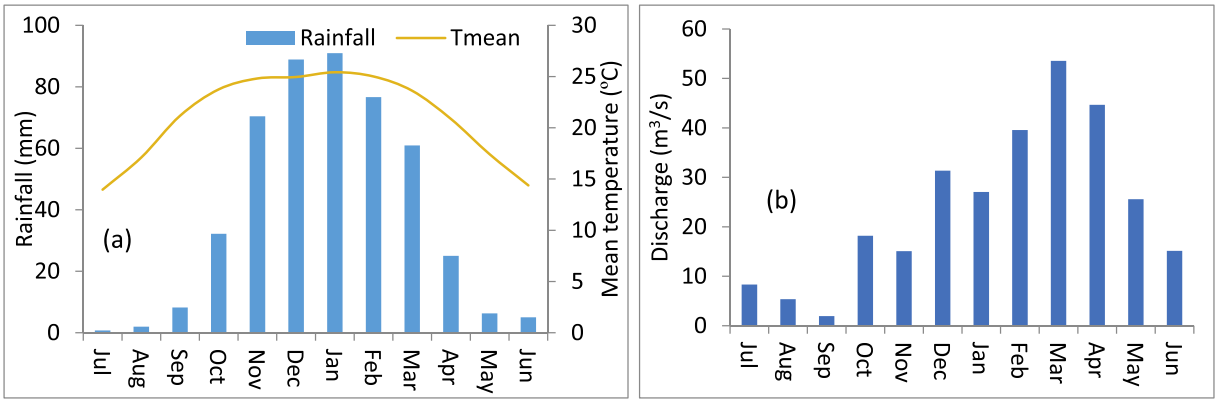

Fig. 3. Monthly climatic and flow data in the Limpopo river system (a) Areal rainfall and mean temperature (b) River Limpopo discharge recorded at Buffel's drift.

indicating a lag between the rain season and generation of flow. For the same reasons as the Okavango river system, analysis that incorporates rainfall, temperature and flow are made to study drought dynamics in this river system.

2.3. Preliminary climatic characteristics

Preliminary analysis of climatic characteristics is done through comparison of decadal rainfall with long term mean over the study period using two representative stations from each of the river systems. This is done to investigate possible shift in rainfall patterns attributed to climate variability in semiarid areas. Rainfall is selected since from studies by Kenabatho et al. (2012), they indicated that changes in other meteorological variables such as temperature, can be revealed through shifting rainfall patterns.

2.4. Determination of hydrological drought index

Hydrological drought is expressed through the standardized flow index (SFI) which takes care of seasonality in the flows other than assuming that hydrological droughts are based on low flow thresholds (Lorenzo-Lacruz et al., 2010; Smakhtin and Hughes, 2004). For Botswana's case, flow is highly seasonal as it is linked to the summer rainfall (GOB-MMEWR, 2006), it requires relating monthly anomalies to long term average conditions (Nalbantis and Tsakiris, 2009; Vicente-Serrano and López-Moreno, 2005). In lieu of this, the study used the procedure of standardization of time series at various timescales of 3-, 6-, 12-, 18- and 24-months to describe hydrological drought dynamics. This procedure has been applied in studies by Byakatonda et al. (2016), Lorenzo-Lacruz et al. (2010), and Shukla et al. (2011). The technique of L-moments is employed to identify the probability density function (pdf) that best fits the flow time series by comparing with various skewed distributions plotted on an L-moment diagram (Byakatonda et al., 2016; Dikgola, 2015; Hosking and Wallis, 2005). From the pdf that best described the flow, a 3-paramter distribution represented by the scale, location and shape of the time series were deduced from the L-moment diagram. This study identified that the Generalized Extreme Value (GEV) function best models the flow data most of the time in the two river systems. This was in agreement with findings of Dikgola (2015) who identified GEV to fit well River Okavango flow time series. The L-moment procedure has been described in Byakatonda et al. (2016). The pdf of the GEV category of a function S representing flow time series according to Hosking and Wallis (2005) is given by;

$$f(S) = \alpha^{-1}\exp[-(1-k)\ y-\ \exp(-y)] \tag{1}$$

Where,

$$y= \begin{cases} -k^{-1}ln\left[1-\frac{k(s-\xi)}{\alpha}\right], & k \neq 0 \\ \frac{(s-\xi)}{\alpha}, & k = 0 \end{cases} \tag{2}$$

The cumulative density function is given by;

$$F(S) = \exp[-\exp(-y)] \tag{3}$$

Where ξ, α, and k are location, scale and shape parameters, respectively, for S ranging from:

$$S: \begin{cases} -\infty < s \leq \xi + \frac{\alpha}{k}\ if\ k > 0 \\ -\infty < s < \infty\ if\ k = 0 \end{cases} \tag{4}$$

The Parameters are computed as a function of L-moment ratios as follows;

Shape parameter,

$$k= 7.859\ c+ 2.9554c^2 \tag{5}$$

Where,

$$c= \frac{2}{3+\tau_3} - \frac{\ln 2}{\ln 3} \tag{6}$$

Scale parameter,

$$\alpha= \frac{\lambda_2 k}{(1-2^{-k})\Gamma(1+k)} \tag{7}$$

Location Parameter,

$$\xi= \lambda_1 - \frac{\alpha[1-\Gamma(1+K)]}{k} \tag{8}$$

Where λ_1, λ_2 and λ_3 are L-moments of order 1, 2 and 3 obtained from flow series. Their derivation have been explained in Byakatonda et al. (2016). Also τ_3 is the L-coefficient of skewness given by;

$$\tau_3 = \frac{\lambda_3}{\lambda_2} \tag{9}$$

The cumulative density function in equation (3) is then standardized to D-values, through an approximation by Abramowitz and Stegun (1964).

The F(S) values were then transformed to a normal variable through the following approximation expressed as;

$$D= M- \frac{A_0 + A_1\ M+ A_2M^2}{1 + B_1\ M+ B_2M^2 + B_3M^3} \tag{10}$$

Where,

$$M= \sqrt{\ln\left(\frac{1}{P^2}\right)} \tag{11}$$

Where P is the probability of exceeding a certain quantile of the flow series obtained from $P = 1 - F(S)$. The constants A and B are given by $A_0 = 2.515517$, $A_1 = 0.802853$, $A_2 = 0.010328$, $B_1 = 1.432788$, $B_2 = 0.189269$, $B_3 = 0.001308$.

The D-index series have an average of zero and standard deviation of one. At every timescale, the hydrological droughts were defined by indices below zero. The value of the index at any point defines the magnitude and intensity of the drought.

2.5. Determination of climatological drought index

The climatological drought index is computed based on the standardized precipiation evapotranspiration index (SPEI) which is a multiscalar drought index (Byakatonda et al., 2016; Lorenzo-Lacruz et al., 2010; Vicente-Serrano et al., 2010) at the same timescales of 3-, 6-, 12-, 18- and 24-months to describe climatic drought dynamics. The SPEI is computed from climatic water balances which is the difference between precipitation and potential evapotranspiration (ETo). The climatic water balances are accumulated at the various timescales, this aids identifiction of different categories of droughts and lags between climatological and hydrological droughts (Khan et al., 2008; Lorenzo-Lacruz et al., 2010; Vicente-Serrano and López-Moreno, 2005). Due to climatological data limitations, the ETo is computed using the Hargreaves method other than the FAO recommended Penman Montheith method. The Hargreaves method has been tested and recommended for use in semiarid environments (Allen et al., 1998; Byakatonda et al., 2018a, 2016; Stagge et al., 2014). The Generalized logistic distribution (GLO) is identified to model the climatic time series using the same procedure of the L-moments described in Section 2.4. Similarly negative values of the index signifies dry conditions and its magnitude a measure of drought severity.

2.6. Association between climatological and hydrological droughts

To assess the inter linkages between climatological and hydrological droughts, statistical analysis were performed. A degree of association is determined through bivariate Pearson's correlation analysis at 5% level of significance. Correlations are determined at each identified timescale to come up with the most suitable period for the respective river systems that could be used in drought monitoring and management. The correlation analysis is done for both monthly (seasonal) and combined drought severity time series. This is handy in investigating seasonality while identifying months of the year with significant association between indices. Evolutions of climatic and hydrological droughts were superimposed to identify time lags that may exist between the two drought classifications. The lags are further confirmed through a lag correlation analysis between climatic and hydrological droughts at timescales of 12-, 18-, and 24-months. This time lag is considered as the period taken for climatological drought to propagate to hydrological drought. To identify the timescale which can be used by operational hydrologists and water managers in Botswana's drought management, plots of probabilities of experiencing a given droughts category against timescale from individual river systems were also superimposed to delineate the region of their interaction. The joint identified timescale for the study area is used to investigate future drought severity variability through rescaled range analysis and modeling using artificial neural network (ANN). Drought occurrence probability is determined from the ratio of the frequency of occurrence of that drought category to the total SPEI events during the historical period (Byakatonda et al., 2016).

2.7. Rescaled range (R/S) analysis of climatic drought index (SPEI)

Drought indices aid understanding of the evolution and dynamics of droughts expressed through their magnitude, duration and intensity. However due to high climate variability in semiarid environments, it is also necessary to determine the extent of variability in drought dynamics. In this study, variability and long term persistence or reversion in the drought dynamics is investigated through rescaled range analysis (R/S) (Sakalauskiene, 2003; Voss, 2013). Linked with rescaled range analysis is the Hurst coefficient (H) which is an expression of long term dependence and also a measure of variability (Granero et al., 2008; Koutsoyiannis, 2003; Sakalauskiene, 2003). The H-coefficient ranges from $0 \leq H \leq 1$, $H > 0.5$ indicates persistence in the time series while $H = 0.5$ is an indicator of randomness in the data. $H < 0.5$ is a sign of reversion in the trend of the time series in the next time period.

Below are the steps undertaken for rescaled range analysis to enable estimation of the H-coefficient;

1. Drought severity at identified timescale for drought monitoring were denoted as a stationery stochastic process D_i with i = 1,2,3, …,N, where i denotes months of length N and D are SPEI values determined from Equation (10).
2. The D_i time series are divided into multiple regions of ranges with varying lengths (i = 1,2,3 … n) with n being length of a given sub series. For this study the data set is split into six ranges of sub series categorized as follows;
   a. First range includes complete drought severity series (n = N)
   b. Second range, data are split into 3 sub series ($n \approx N/3$)
   c. Third range data are split into 6 sub series ($n \approx N/6$)
   d. For the fourth range, the time series are divided into 12 sub series of equal length ($n \approx N/12$)
   e. Fifth range data are divided into 24 multiple units ($n \approx N/24$)
   f. For the last range, series are split into 48 different series ($n \approx N/48$)
3. The expected values ($\overline{D}$) of each of the time series above is then determined
4. The expected value from 3 above for each range is used to generate series of deviations as follows; $Y_i = D_i - \overline{D}$ for i = 1,2,3 … n
5. The minimum and maximum values from the deviation series are then determined. An adjusted range is computed from $R^* = Max(Y_1, Y_2 ... Y_n) - Min(Y_1, Y_2 ... Y_n)$
6. The standard deviation (SD) for each range is then computed
7. The rescaled range is computed from $R/S = \frac{R^*}{SD}$, for each sub range an average R/S is computed.
8. Rescaled range is related to H-coefficient through $(R/S) \approx kn^H$
9. The H-coefficient is then obtained by running a regression following the expression,

$$\ln\left(R/S\right) = \ln(k) + H.\ \ln(n) \tag{12}$$

10. A slope of the regression plot of ln(R/S) against ln(n) results in the H-coefficient, which is a measure of variability in the time series while at the same time describing the long term dependence process of D_i series.

This procedure has been applied in studies of trends in hydrological time series and financial markets (Granero et al., 2008; Munshi, 2014; Sakalauskiene, 2003; Voss, 2013).

2.8. Nonlinear autoregressive with exogenous input (NARX) neural network model

Neural networks comprises of inter linkages of process nodes that enable learning of input and output processes (Byakatonda et al., 2018a, 2016; Masinde, 2014; Rajasekaran et al., 2011). To develop future drought dynamics situations, the NARX model is utilized. The NARX model is a class of recurrent neural network (RNN) equipped with tapped delay lines that provides additional dynamic memory to aid learning of complex nonlinear multivariate processes. The network comprises of an input and output regressor with feedback connectors

from the output layer for better learning and eventual generation of dynamic patterns of drought severity. The NARX forecasting building process involves the following:

1. Data preprocessing by conveniently selecting the exogenous inputs known to affect the outcome and behavior of the target series,
2. Selection of the model architecture,
3. Training and learning of the model in an open loop mode and
4. Generation of model forecasts in a closed loop mode.

2.8.1. Data preprocessing

Input and target series were rescaled to range between −1 and 1 through the MAPMINMAX option in the MATLAB TOOLBOX. This standardized range makes mapping of the inputs and targets easier since they are within the same range. The data is then divided in the ratio 70:15:15 for training, validation and model testing respectively using the dividerand() option. The NARX model for m steps ahead forecast is represented by

$$\hat{T}(t+ m) = f[\hat{T}(t+ m- 1), ...,\hat{T}(t+m-i); X(t)] \quad (13)$$

Where X(t) the input vector also acts as the exogenous input to the model while T(t + m) is the target series output at time step t. For this study the input vector used comprised of monthly rainfall, minimum and maximum temperature while f(.) is a nonlinear mapping function, i = 1,2,3 … number of memory delays. At the input regressor, T(t + m-i) acts as the autoregressive component of the model.

2.8.2. Nonlinear autoregressive with exogenous input (NARX) model architecture

The model is comprised of an input regressor, one hidden layer and an output layer. The model selected is made of 11 neurons in the hidden layer with maximum delay of 4. This selection is based on the performance involving various ANN configurations. In the simulation mode the model feeds back the output to the autoregressive component of the model to generate new outputs. The model architecture is presented in Fig. 4.

2.8.3. Training of the ANN model

The model is trained in a series-parallel connection (Open loop) in which only actual values of the target series are fed at the output's regressor. The mathematical model in Equation (13) is modified during training to;

$$\hat{T}(t+1) = f[T(t), ...,T(t+1-i); X(t)] \quad (14)$$

In this mode, the network performs a onestep ahead forecast that is fed back to the output's regressor until m steps ahead forecasts are obtained. The model trains without m most recent actual targets and inputs. These m values are stored and used for validation of the forecasts. For every input to the model, there is a corresponding output. To minimize the errors between this output and the actual target series, the Levenberg-Marquardt (LVM) algorithm is utilized. The LVM is a back propagation algorithm which adjusts weights and biases of the network in order to minimize the errors. The network also uses sigmoid and linear type transfer functions at the hidden and output layers respectively.

2.8.4. Drought severity forecast with artificial neural network (ANN)

The trained network makes m steps forecast in a parallel mode (Closed loop) using Equation (13). The actual targets at the input are gradually replaced by new forecasts in a recursive manner until m steps forecasts are achieved. For this study 60 months forecasts were made. Performance evaluation of the network is through the mean square error (MSE) and coefficient of determination between the actual targets and the output targets.

3. Results

3.1. Preliminary rainfall characteristics

To confirm the shift in the climatic regime as reported by earlier studies and their statistical significance, the homogeneity tests in Section 2.2 are used. Tests on annual rainfall series at the six synoptic stations did not indicate any statistical significance in the shift (Table 1) by all the three tests. For this reason, the complete period of the data record (1975–2014) is used in the analysis.

Further analysis of rainfall characteristics from Shakawe and Mahalapye located in Okavango and Limpopo river systems respectively reveals high variability during summer months of November to April. Decadal rainfall mass curves (Fig. 5) also indicate that, there has been only one decade where above long term average rainfall is experienced (1975–1984). In the recent past either average or below average rainfall is observed at the two representative stations from each of the river systems. It is also evident from Fig. 5 that the biggest contribution of rainfall is registered during summer.

In lieu of rainfall variability especially during the summer period compounded by declining totals, it becomes necessary for this study to investigate the evolution of climatological and hydrological droughts at various timescales to facilitate early warning strategies.

3.2. Dynamics of climatic and hydrological droughts

Dynamics of climatic and hydrological droughts have been plotted on the same scale and presented in Fig. 6 and Fig. 8 for the Limpopo and Okavango river systems respectively. Climatic droughts were derived from Selibe-Phikwe, Mahalapye and SSKA synoptic stations located in the Limpopo river system while for the Okavango river system, Kasane, Maun and Shakawe were used. Both wet and dry spells have been recorded on the plots. Drought dynamics at shorter timescales of 3- and 6-months are more frequent than those at higher timescales of 18- and 24-months. The dynamics of hydrological droughts show similar pattern though with a lag at both river systems. For both drought dynamics, negative standardized values signify dry conditions while positive values humid periods. In the Limpopo river system flow data was available for a period between 1997 and 2014, to facilitate comparison with climatic droughts, analysis is made over this period. In this river system, a dry spell between 2000 and 2003 was recorded by climatic dynamics, during the same period low flows were also recorded between 2002 and 2004 though with less severity. The next dry period recorded by the climatic dynamics is that between 2006 and 2007 with below average flows ensuing between 2008 and 2009. A period from 2011 to 2013 was also characterized by climatic drought which was followed by low flows between 2012 and 2013. However the low flows during this period were of a shorter duration compared to climatic droughts. Wet spells in the Limpopo river system were equally registered with the period between 1998 and 2000 characterized by wet spells with above average flows registered during 1999/2000. The next wet spell on record was that between 2008 and 2009 with high flows following between 2009 and 2010. Another mild wet spell that has been recorded is between 2013 and 2014 which was followed by above average flows during the first half of 2014. From these dynamics, it is observed that at lower timescales both drought dynamics align together with lags more pronounced at higher timescales of 12-, 18- and 24-months. In the Limpopo river system, an average of 7 months lag between climatic and hydrological droughts is observed indicated as L_l in Fig. 6d. The lag correlation plot (Fig. 7a) further confirms this lag. Lag correlations shown in Fig. 7a are observed to steadily increase from lag 1 until 7 months for the 12- and 18-months correlations. Beyond 7 months a sudden drop in correlation is observed. For the 24-months timescale, the decline starts earlier at 6 months lag. This may be regarded as the time taken for meteorological drought to propagate to hydrological drought. Analysis of linear trends indicates increasing

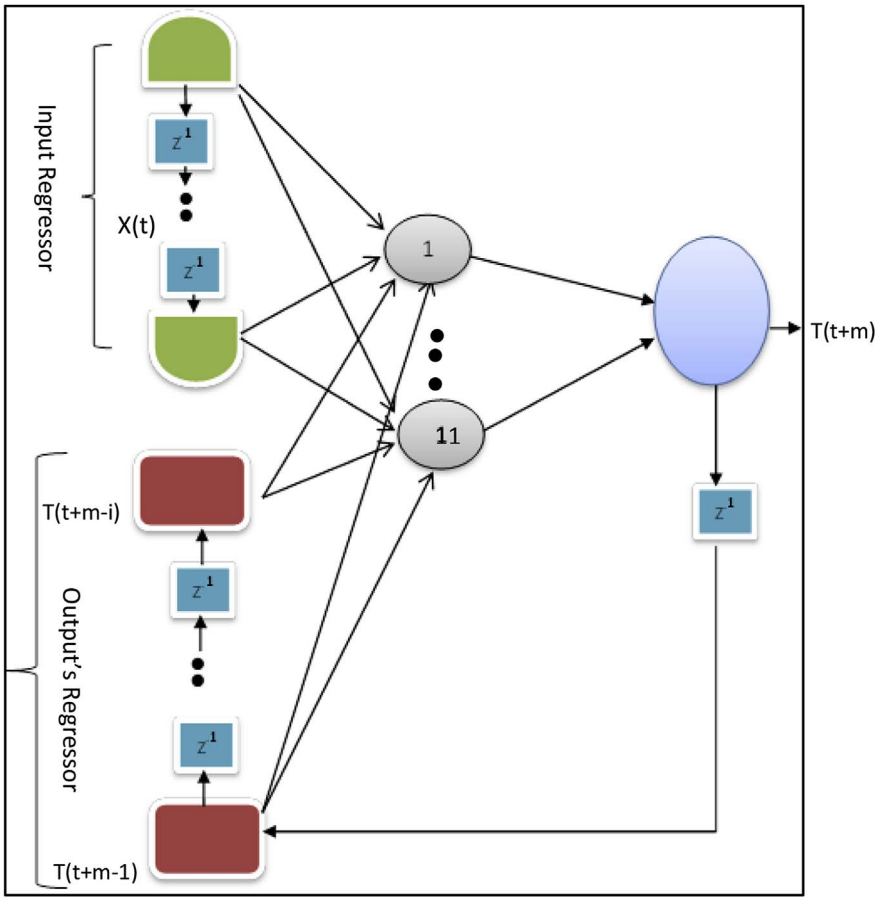

Fig. 4. Nonlinear autoregressive with exogenous input (NARX) neural network model architecture with process nodes.

Table 1
Annual Rainfall (1975–2014) p-values from the three homogeneity tests.

SN	Station name	Pettit's test	SNHT	BHD's test
1	Kasane	0.08	0.07	0.10
2	Mahalapye	0.55	0.60	0.52
3	Maun	0.31	0.26	0.13
4	Selibe-Phikwe	0.65	0.45	0.50
5	Shakawe	0.71	0.93	0.74
6	SSKA	0.47	0.36	0.56

Test is significant at 5% level.
SNHT = standard normal homogeneity test and **BHD** = Buishand test.

gradient towards drying conditions across the Limpopo river system with the drying gradient increasing at higher timescales. Linear trends expressed as a percentage of Z-units were −0.06%, −0.07%, −0.13% and −0.29% at time scales of 3-, 6-, 12- and 18-months respectively as shown in Fig. 6d. These negative trends are towards drying conditions that are increasing across timescales in the Limpopo river system. The dynamics of the 24-months timescale are not presented because they were similar to those at 18-months.

In the Okavango river system, also the general patterns of dry and wet spells recorded by dynamics of climatic drought were not different from those observed in the Limpopo river system. Flow data in the river system was available from 1975 to 2014. The dry spell from 1981 to 1984 that was recorded throughout the study area is also registered by the dynamics of droughts. The below average flows started earlier in 1980 as it emanated from another mild dry spell that had occurred during the period of 1979/80 season. These low flows normalized in 1983. Another dry spell recorded by the climatic dynamics is between 1990 and 1993 with hydrological drought closely following between

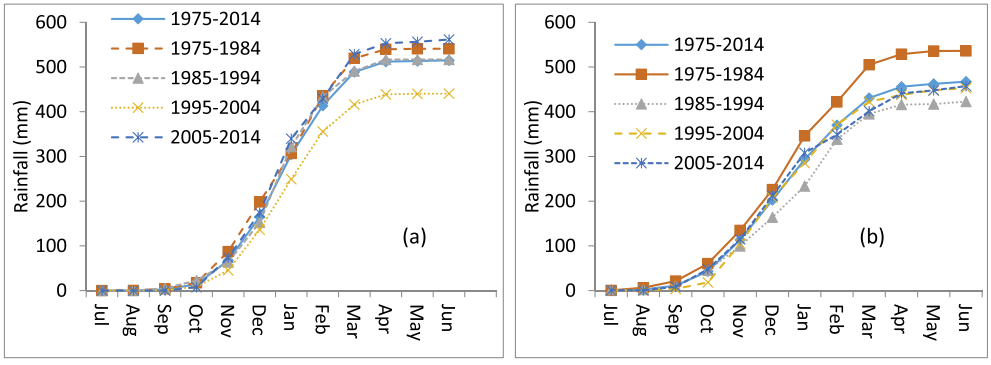

Fig. 5. Comparison of decadal and long term rainfall (1975–2014) mass curves (a) Shakawe (b) Mahalapye.

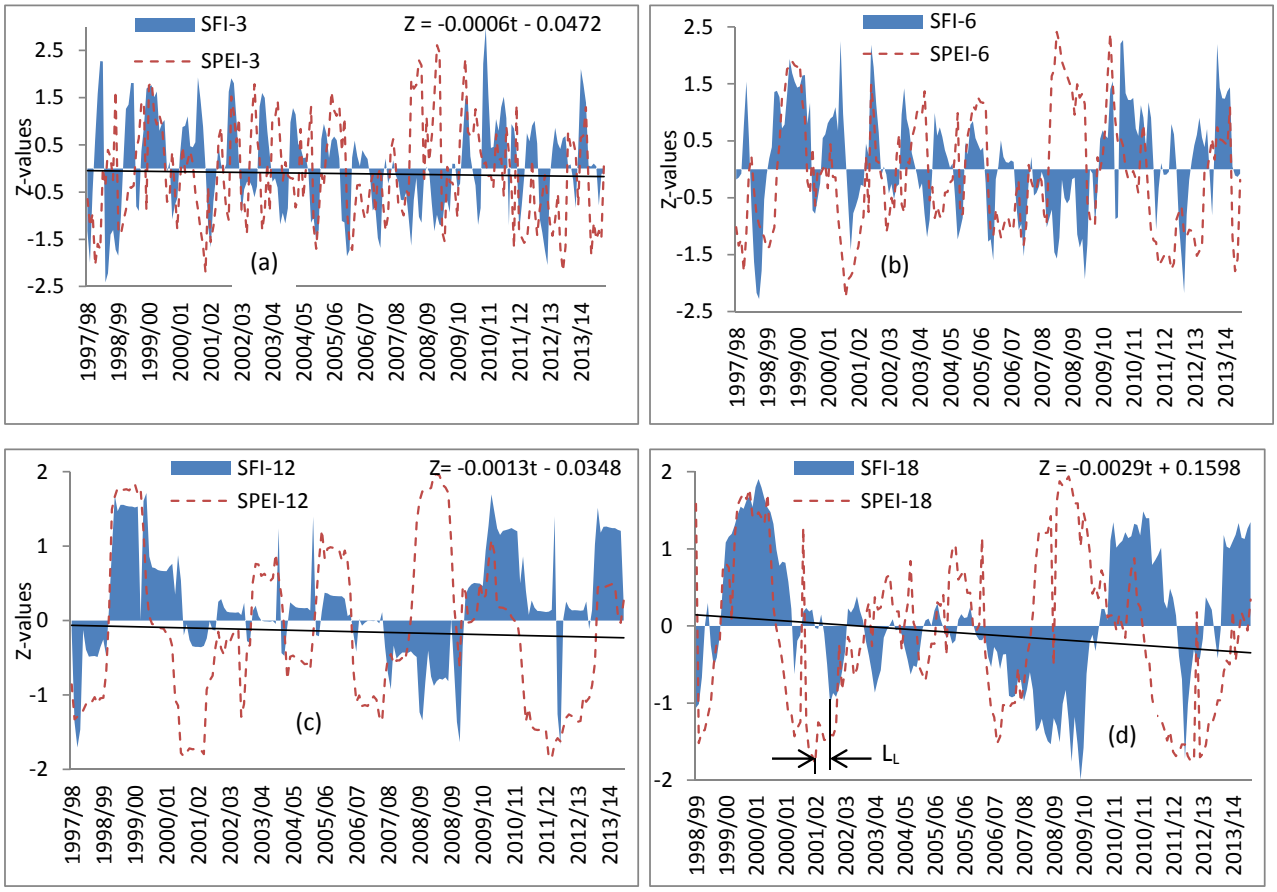

Fig. 6. Dynamics of climatic (dotted red) and hydrological (shaded blue) droughts in the Limpopo river system at timescales of a) 3-months, b) 6-months, c) 12-months and d) 18-months. (For interpretation of the references to colour in this figure legend, the reader is referred to the Web version of this article.)

1992 and 1994. Further still between 1994 and 1996, climatic droughts recorded a dry spell together with low flows in the same year whose effects had accrued from the previous period but normalized in 1998. The subsequent dry spells registered by climatic drought were between 2002 and 2003 with a short punctuation but resumed shortly in 2004 until 2006. These dry spells did not result into significant flow reduction due to the wet spells that had been recorded between 2000 and 2002.

Wet spells and above average flows in the Okavango river system were also registered by both climatic and hydrological droughts respectively. A wet spell which was registered between 1988 and 1990 did not generate high flows due to the prolonged drought in the previous period of 1981–1984. A wet period between 2009 and 2011 resulted into the highest flows recorded during the historical period from 2009 to 2013. As the case in the Limpopo river system, climatic and hydrological drought dynamics are found to align at lower timescales. At higher timescales of 12-, 18- and 24-months, it takes an average of 6 months for meteorological droughts to propagate to hydrological droughts in the Okavango river system. This is indicated as L_o in Fig. 8d and confirmed with the lag correlation plot in Fig. 7b. Linear trends indicate a constantly increasing gradient towards dry conditions of 0.20%, 0.16% and 0.18% at 3-, 12-, 6- and 18-months respectively. There is no observed pattern of drought trends across timescales in the Okavango river system as was the case for Limpopo.

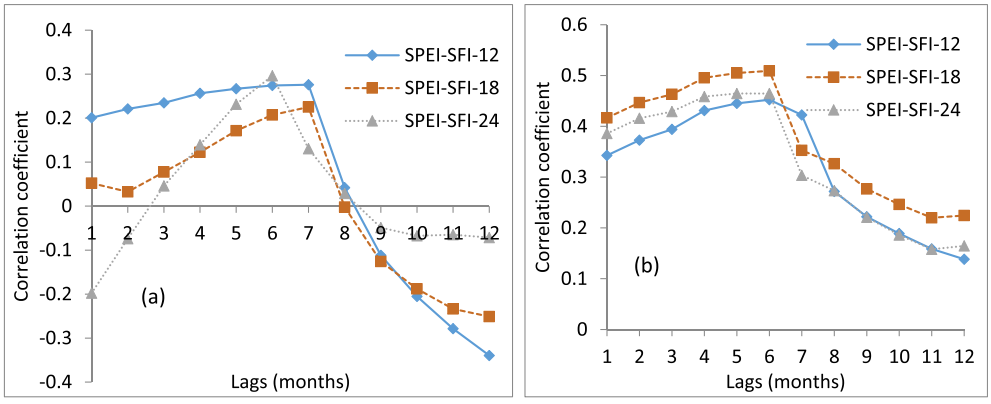

Fig. 7. Lag correlations between climatic and hydrological drought severities at timescales of 12-, 18- and 24-months at (a) Limpopo and (b) Okavango.

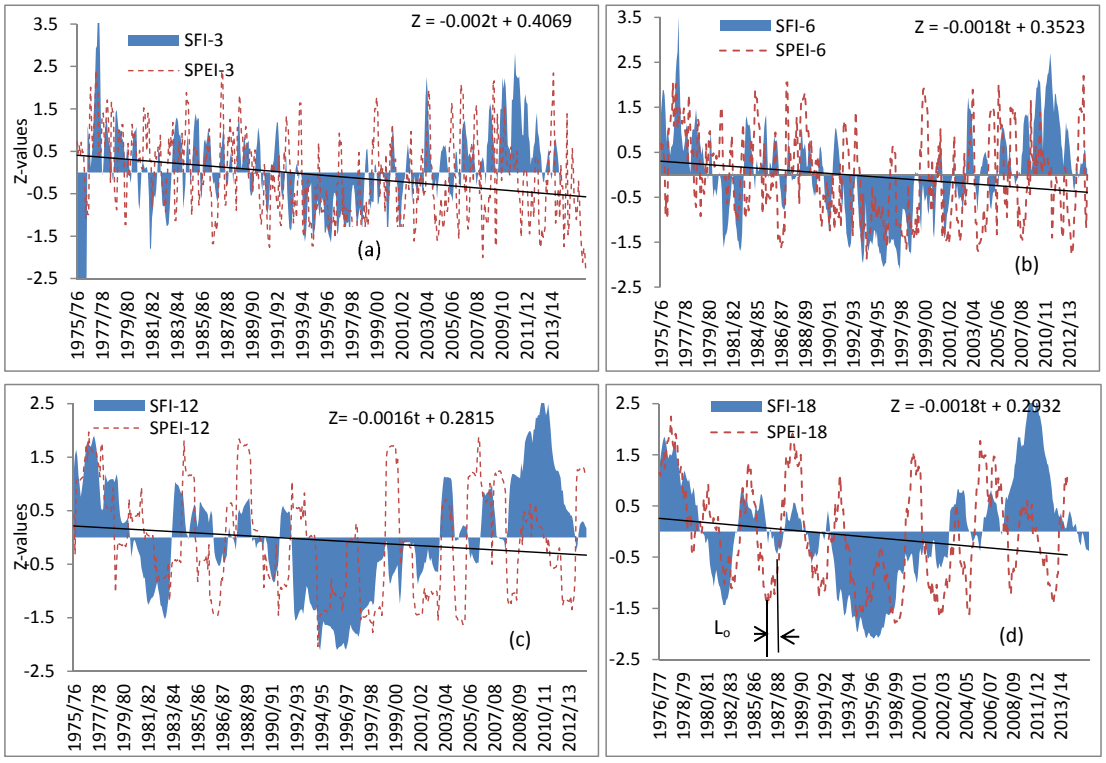

Fig. 8. Dynamics of climatic (dotted red line) and hydrological droughts (shaded blue) in the Okavango river system at timescales of a) 3-months, b) 6-months, c) 12-months, and d) 18-months.

3.3. Degree of association between climatic and hydrological droughts

The degree of association has been analyzed for both the combined and monthly series between climatic and hydrological drought indices. Results from this analysis are presented in Table 2. Analysis of monthly series is instrumental in understanding the seasonal behavior of the drought dynamics. In the Limpopo river system, significant correlations are observed in March and April at 3-months timescale. At 6-months timescale, significant correlations occur in February, March, April, May, June and July. For the 12-months timescale, the only significant correlation is registered at the end of the summer rain season in March. The 18- and 24-months timescale shows no significant positive correlations across the entire period. The combined series show similar trends as the monthly series. The degree of association for these series increases across timescale with a maximum of 0.25 occurring at 12-months and declining in the subsequent timescales. None of the correlations is significant at 95% confidence level for the combined time series of the indices in the Limpopo river system.

Correlations from the Okavango river system also presented in Table 2 indicate significant correlations in June, July, August, September, October and November at 3-months timescale. At 6-months, significant correlations were recorded in August, September, October and November. 12-months timescale had January, February, March, October and December also registering significant correlations. At higher timescales of 18- and 24-months, all correlations across the entire period were positive and significant. For the combined series, correlations increased across timescale with the lowest of 0.27 and a highest of 0.42 recorded at 3- and 18-months in the Okavango river

Table 2
Correlation coefficient between climatic and hydrological droughts.

Month	Timescale									
	Limpopo					Okavango				
	3	6	12	18	24	3	6	12	18	24
January	−0.09	0.01	0.20	−0.03	−0.07	0.32	0.33	0.38[a]	0.44[a]	0.50[a]
February	−0.14	0.45[a]	0.26	0.14	−0.22	0.26	0.31	0.47[a]	0.42[a]	0.48[a]
March	0.63[a]	0.62[a]	0.43[a]	0.07	−0.17	0.01	0.22	0.36[a]	0.41[a]	0.44[a]
April	0.62[a]	0.50[a]	0.30	0.12	−0.36	0.02	0.20	0.29	0.42[a]	0.41[a]
May	0.27	0.41[a]	0.33	0.10	−0.38	0.28	0.19	0.29	0.39[a]	0.41[a]
June	−0.07	0.39[a]	0.29	0.17	−0.39	0.35[a]	0.22	0.30	0.42[a]	0.41[a]
July	−0.18	0.41[a]	0.30	0.05	−0.40	0.28	0.27	0.31	0.42[a]	0.43[a]
August	−0.15	0.03	0.31	0.10	−0.39	0.37[a]	0.45[a]	0.33	0.45[a]	0.43[a]
September	−0.06	−0.12	0.30	0.08	0.37	0.34[a]	0.45[a]	0.33	0.43[a]	0.44[a]
October	−0.04	0.06	0.25	0.18	−0.37	0.36[a]	0.35[a]	0.35	0.40[a]	0.45[a]
November	−0.21	−0.01	0.11	0.13	−0.30	0.47[a]	0.36[a]	0.33	0.41[a]	0.43[a]
December	−0.20	−0.22	−0.05	0.05	−0.09	0.31	0.33	0.33	0.41[a]	0.42[a]
Combined time series	**0.02**	**0.18**	**0.25**	**0.07**	**−0.22**	**0.27**	**0.31**	**0.34**[a]	**0.42**[a]	**0.39**[a]

[a] Significant at 95% confidence level.

Table 3
Drought categories with their probability of occurrence.

Class	Drought Classification	Limpopo					Okavango				
		SPEI-3	6	12	18	24	3	6	12	18	24
< -2	Extremely Drought	0.0	0.0	0.0	0.0	0.0	0.0	0.0	0.0	0.0	0.0
−1.99 to −1.50	Severe Drought	4.0	4.0	4.0	4.0	4.0	4.0	4.0	3.0	5.0	6.0
−1.49 to 1.00	Moderate Drought	12.0	13.0	13.0	16.0	17.0	14.0	15.0	17.0	13.0	13.0
−1.00 to 1.00	Near Normal	65.0	65.0	64.0	61.0	59.0	65.0	62.0	60.0	60.0	56.0
1.00 to 1.49	Moderate Wetness	11.0	11.0	10.0	10.0	9.0	10.0	13.0	12.0	14.0	16.0
1.50 to 1.99	Severe Wetness	5.0	6.0	8.0	7.0	8.0	5.0	5.0	7.0	6.0	6.0
> 2.00	Extreme wetness	2.0	1.0	0.0	0.0	0.0	2.0	1.0	0.0	0.0	0.0

system. Generally the Okavango river system is significantly affected by droughts at higher timescales compared to the Limpopo river system.

3.4. Timescale for drought monitoring across Limpopo and Okavango river systems

To facilitate drought monitoring and mitigation across the two river systems, a common timescale is required to guide operational hydrologists and users of water resources within these river systems. Drought monitoring is directly linked to the degree and extent of vulnerability. Droughts have been categorized according to classification by Byakatonda et al. (2016) and given in Table 3. Droughts are classified as extreme, severe and moderate across all the timescales. Probabilities of occurrence of a drought event are determined from the frequency of drought per category as indicated in the classification in Table 3. This is also taken as a degree of drought vulnerability towards that drought category. Results of these probabilities of occurrence are presented in Table 3. From these results, moderate followed by severe droughts are the most common across the study area. Extreme droughts are a rare occurrence with negligible probabilities recorded at both river systems for all the timescales.

The highest probability of 17% for moderate drought is recorded at 24-months timescale in the Limpopo river system. The same degree of vulnerability was registered in the Okavango river system but at a lower timescale of 12-months. For severe droughts, a probability of 4% is recorded in the Limpopo river system across timescales. In the Okavango river system, severe droughts registered the highest probability of 6% at 24-months timescale. Since Botswana has been identified in Table 3 to be more vulnerable to moderate droughts than any other drought category, this study uses moderate drought probabilities across the two river systems to establish that common timescale that can be used in monitoring. To achieve this, the probability of occurrence of this drought category is plotted against timescale for both river systems on the same axis as shown in Fig. 9. The results indicate that, vulnerability increases with timescale in the Limpopo river system. In the Okavango river system the plot indicates that vulnerability increases steadily reaching the peak at 12-months timescale. These results further reveal that the Okavango river system is more vulnerable to moderate droughts than the Limpopo river system up to 15-months timescale. A common timescale established from this analysis across the two river systems is 15-months that can be useful in joint drought monitoring. The variability in drought dynamics at this common timescale needs to further be investigated to reveal possible future changes that might affect water resources in these river systems.

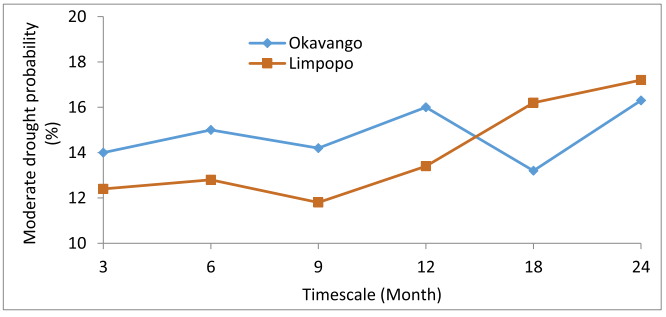

Fig. 9. Probability of moderate drought occurrence across timescales.

3.5. Rescaled range analysis of climatological droughts at 15-months timescale

Standardized precipitation evapotranspiration index (SPEI) combined time series at timescale of 15-months are further analyzed for the two river systems. This is to establish the extent of variability in the drought dynamics at this timescale and at the same time check for possibility of persistence or reversion using the Hurst coefficient as a drought monitoring mechanism. Results of the relationship between rescaled range and rescaled sample size are presented in Fig. 10. These results reveal H-coefficients of 0.06 and 0.08 in the Limpopo (Fig. 10a) and the Okavango (Fig. 10b) river systems respectively. These coefficients being significantly less than 0.5, indicates high variability in the dynamics and a possibility of a reversion in these dynamics in the near future. However this does not give the magnitude of the change that is required for operational purposes. For this reason it is necessary to perform forecasts that will provide this magnitude over a given planning horizon.

3.6. Climatological drought forecasts at 15-months timescale using NARX-ANN model

A 15-months timescale was identified in Section 3.4 to adequately monitor drought dynamics in Botswana. Attempts were made to investigate futuristic behavior of drought dynamics at this timescale through the Hurst phenomena. The results indicated high variability and possible reversion in the dynamics. It was hence necessary to quantify the future drought dynamics through forecasts provided by the NARX neural network model. Results from the NARX model for development of future drought dynamic conditions are presented in Fig. 11. These results indicate that the NARX network is effective in learning the relationship between the inputs and the targets to produce an output that closely matched the actual targets. The model returned high performance in terms of the coefficient of determination (R^2) between the actual targets and the outputs. The model returned an R^2 of 0.94 at both locations of Okavango and Limpopo. Performance in terms of MSE, Okavango returned an error of 0.058 while at Limpopo it was 0.060.

At the end of the observed period, the Okavango (Fig. 11a) is experiencing moderately dry conditions while in the Limpopo (Fig. 11b) conditions are moderately wet. At the beginning of the forecast period, indeed a reversion in the current conditions is seen to take place. At the Okavango river system, it is observed that the month following the observed period forecasted a moderately wet period while at the Limpopo, forecasts indicate a gradual change towards dry conditions. At both locations, the forecasts project generally dry conditions for the

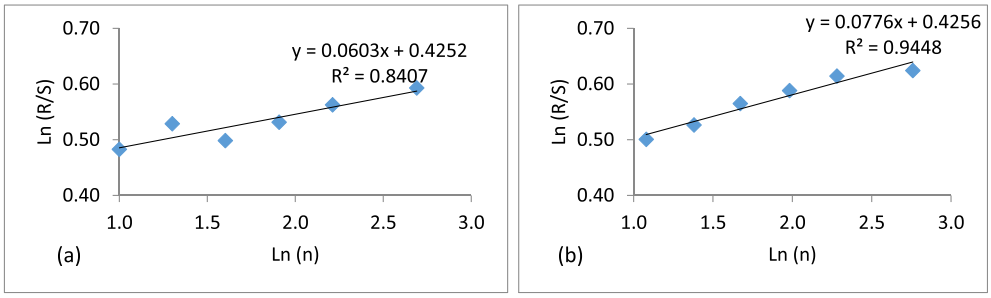

Fig. 10. H-Coefficients for the two river systems (a) Limpopo (b) Okavango.

next 40 months, and thereafter, conditions towards normal are expected.

4. Discussion

4.1. Dynamics of climatic and hydrological droughts

The dynamics of climatic and hydrological droughts presents with differing frequencies at various timescales. For the shorter timescales, the wet and dry periods are more frequent with no distinct spells observed. The closer alignment of dynamics of climatic and hydrological droughts at lower timescales could be attributed to the high frequency in variation between wet and dry episodes. This limits the time of expression of possible lags between these events. Besides, at lower timescales hydrological droughts are highly unlikely since at 3-months, agricultural droughts are the ones at play as demonstrated in a number of studies on drought propagation by Mishra and Singh (2010), Van Loon (2013) and Trambauer et al. (2014). These finding are equally in agreement with those reported by Lorenzo-Lacruz et al. (2010) and Nalbantis and Tsakiris (2009) who reiterated similar behavior from related studies in Spain and Greece respectively. Drought trends reveal drying conditions which may threaten livelihood activities derived from these river systems. These two river systems are the main source of water resources for Botswana. Okavango is a delta recognized as Ramsar site and Limpopo is host to majority of the surface dams that supply water for both domestic and industrial needs. Okavango river system equally hosts most of the commercial farms that supplies majority of the food demand. Therefore it is necessary to develop these early warning systems to assist in drought mitigation measures. From the drought dynamics, the study also has shown that hydrological droughts lag climatic droughts by 7 months in the Limpopo river system and 6 months in the Okavango river system. This revelation is handy in drought prediction for planning purposes. The study also reveals that Botswana is more prone to moderate droughts than any other category

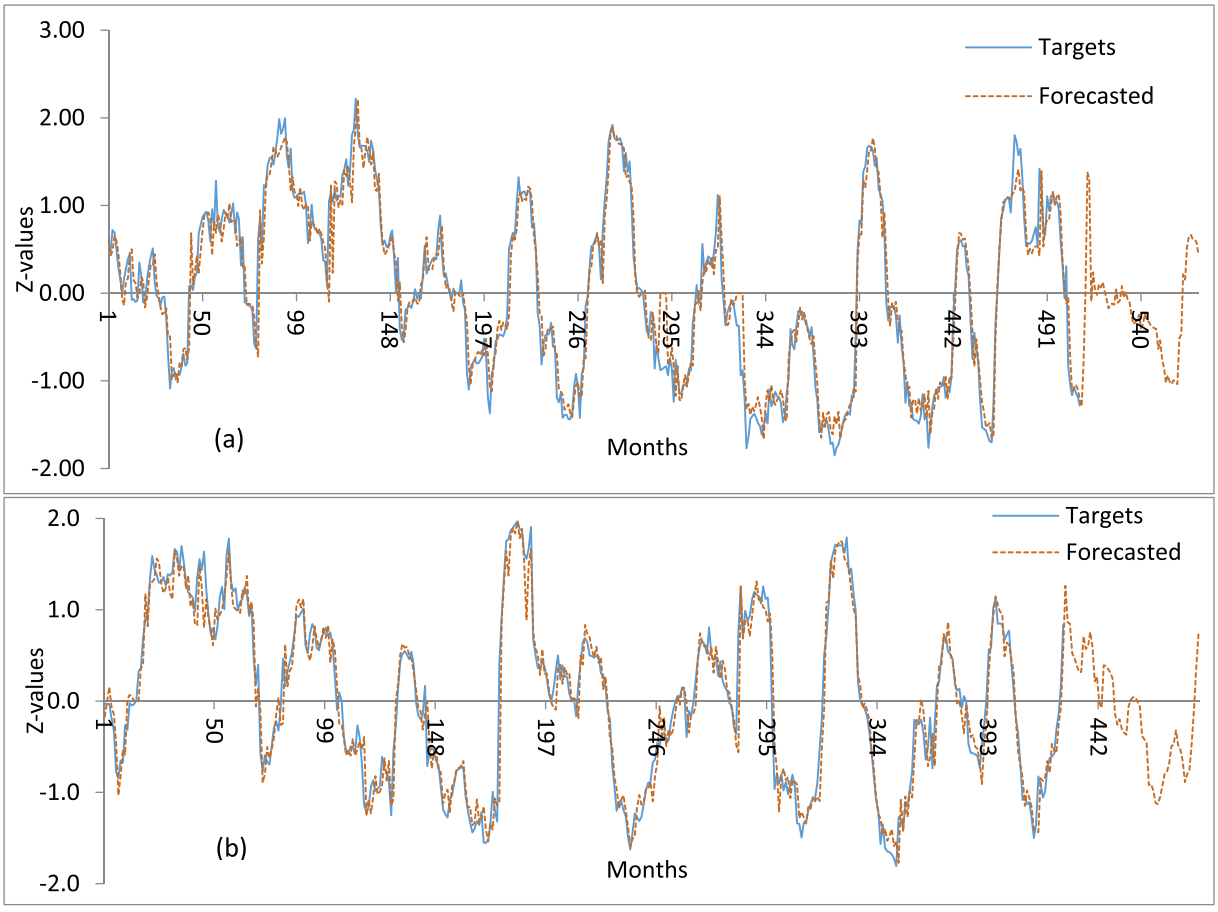

Fig. 11. Comparison of actual targets and forecasted climatic drought severity for SPEI-15 (a) Okavango (b) Limpopo.

of droughts. This finding is in agreement with Zhang et al. (2009) who found moderate droughts to be dominant in the Pearl river system in China. The drought and wet episodes reported by climatic droughts are also expressed by the hydrological drought dynamics though with a lag. Dry periods are recorded across the study area from 1981/82 to 1986/87 repeated in 1994/95 to 1998/99. These drought years were also reported by Masih et al. (2014) which is a demonstration that these indices can adequately capture historical droughts. The dry episodes also coincided with El Niño years of 1982/83 and 1997/98 (Golden gate Weather Services, 2017). Similarly a wet spell recorded over the study area of 1975/76 to 1979/80 also was preceded by La Niña year of 1973/74 (Golden gate Weather Services, 2017). This revelation could link drought dynamics in Botswana to El Niño southern oscillation (ENSO) influences of the Equatorial Pacific. The most recent studies by Byakatonda et al. (2018a,b) as well reported that the local climate is highly associated with the southern oscillation index (SOI). This could be a further confirmation that indeed ENSO influences climate across the study area.

4.2. Degree of association between climatic and hydrological droughts

This study has shown a clear relationship between climatic and hydrological droughts over the study area at varying timescales. In the Okavango system it is evident that hydrological responses increased at higher timescales. This may be explained by the fact that the Okavango river system is an inland delta and as such it acts as storage of river discharge over long periods of time. Lorenzo-Lacruz et al. (2010) in their study found greater responses at higher timescales in Spain for reservoir storage as compared to inflows which showed higher response at shorter scales. Drought in storage mediums depends on amounts previously impounded, implying existing drought conditions are a result of a combined effect of earlier conditions (either wet or dry years). In the Limpopo river system, longer timescales are found not useful in monitoring droughts. Higher responses are found at lower timescale in agreement with similar studies carried out in Greece by Nalbantis and Tsakiris (2009) and Spain by Vicente-Serrano and López-Moreno (2005). The high response at short timescales in the Limpopo river system could be attributed to arenosols with limited moisture storage capacity that dominate the study area (FAO, 2001). At long dry periods, the soils do not have sufficient storage to contribute to stream flow hence the poor response at longer timescales. Comparing Okavango and Limpopo river systems in terms of response, the earlier case can be treated as storage whereas the later as normal river flow. This explains the different responses at various timescales. There was observed seasonal variations in response for the Limpopo river system with significant correlations registered in the months of February, March and April at 3-months timescale. This time period coincides with Botswana's summer rain season. 3-months SPEI in March is an accumulation of moisture deficit for January, February and March, which period covers majority of the rain season. The high correlations are due to the fact that during the months of March and April there is adequate moisture available for atmospheric circulation. The SPEI-6 is also an accumulation of moisture over the six month period which is a summation of the entire summer rain season. Due to the same reasons as SPEI-3, significant correlations were observed during the months of February, March, April, May, June and July for SPEI-6. The same reason is also advanced for the significant correlation in March at 12-months timescale. These seasonal variations are not observed in the Okavango for the reasons that may be related to it being a river delta.

4.3. Rescaled range analysis of climatological droughts at 15-months timescale

Rescaled range analysis with wide application in hydrological studies and financial time series analysis reveals high variability and a possible reversion in the climatic drought dynamics expressed through the H-coefficient close to zero. The use of rescaled range analysis in the study of capital markets has proposed other modifications for calculating the H-coefficient (Granero et al., 2008). This is necessary for testing randomness in the capital market returns. However in this case with a near zero H-coefficient, the possibility of having randomness in the drought dynamics is very minimal across the study area and hence the original method proposed by Hurst (1951) is sufficient in investigating the variability and reversion tendency of drought dynamics in the Botswana case. The very low H-coefficient could also signify high climate variability which is a common feature in semiarid areas that has also been widely reported in numerous studies in the region (Batisani, 2012; Byakatonda et al., 2018a; Moalafhi et al., 2012; Moeletsi and Walker, 2012; Richard et al., 2000).

4.4. Climatological drought forecasts at 15-months timescale using NARX-ANN model

The NARX model has demonstrated its ability to forecast drought severity with help of appropriate exogenous inputs. This demonstration is based on the high performance levels exhibited by the model. The model confirmed the results of $H < 0.5$ indicating a reversion of existing conditions at both river systems. The model forecasts of dry conditions for the next 40 months may even be heightened by strong El Niño conditions experienced in 2015/2016 (Hansen et al., 2016). This agreement in results from rescaled range analysis and ANN shows the ability of combining the two techniques in studying climate variability while at the same time generating forecast to facilitate better management of hydrological systems.

5. Conclusions

This study focused mainly on identifying the timescales at which various components of the hydrological cycle especially stream flow responds to climate variability. A common timescale for drought monitoring has been identified for Botswana as part of drought mitigation strategy. The study was also able to establish drought trends and their variability. From the foregoing analysis and discussion in Sections 3 and 4, the study reveals the following conclusions;

1. The dynamics of droughts show increasing trends in both Limpopo and Okavango river systems towards drying conditions. Climatic droughts were found to take 7 months to propagate to hydrological droughts in the Limpopo river system and the same process takes 6 months in the Okavango river system.
2. Correlations between climatic and hydrological droughts are mainly significant in March and April reaching the peak at 12-months timescale in the Limpopo river system. These correlations were found to increase across timescales for the Okavango river system. A common timescale of 15-months was identified to be suitable for drought monitoring in Botswana. At the identified timescale of 15-months, H-coefficients of 0.06 and 0.08 resulted in the Limpopo and Okavango river systems respectively which is an indication of high variability in drought dynamics. These coefficients also reveal a possible reversion in the existing conditions.
3. The Nonlinear autoregressive with exogenous input (NARX) neural network model forecasts confirm a reversion reported by the H-coefficient and further reveals generally dry conditions for the next 40 months with recovery to normal conditions expected in the last 20 months of the forecast period. The influence of ENSO episodes in the Equatorial Pacific on drought dynamics may not be ruled out.

Acknowledgements

The authors acknowledge support from the Mobility for Engineering Graduates in Africa (METEGA) and Office of Research and Development (ORD) at University of Botswana for funding this study. The

Departments of Meteorological Services (DMS) and Water Affairs (DWA) of Botswana are acknowledged for meteorological and flow data sets respectively used in this study. Gratitude also goes to the editor and anonymous reviewer for their valuable comments that have greatly improved this manuscript.

References

Abramowitz, M., Stegun, I.A., 1964. Handbook of mathematical functions: with formulas, graphs, and mathematical tables. Courier Corporation 55.

Alexandersson, H., 1986. A homogeneity test applied to precipitation data. J. Climatol. 6, 661–675.

Alexandersson, H., Moberg, A., 1997. Homogenization of Swedish temperature data. Part I: homogeneity test for linear trends. Int. J. Climatol. 17, 25–34.

Allen, R.G., Pereira, L.S., Raes, D., Smith, M., 1998. FAO Irrigation and drainage paper No. 56. Rome Food Agric. Organ. United Nations 56, 97–156.

Batisani, N., 2012. Climate variability, yield instability and global recession: the multi-stressor to food security in Botswana. Clim. Dev. 4, 129–140.

Bazza, M., 2002. Water resources planning and management for drought mitigation. In: Regional Workshop on capacity building on Drought Mitigation in the Near East, Rabat (Morocco), 1–5 Nov 2002.

Buishand, T.A., 1982. Some methods for testing the homogeneity of rainfall records. J. Hydrol 58, 11–27.

Byakatonda, J., Parida, B.P., Kenabatho, P.K., Moalafhi, D.B., 2018a. Influence of climate variability and length of rainy season on crop yields in semiarid Botswana. Agric. For. Meteorol. 248. http://dx.doi.org/10.1016/j.agrformet.2017.09.016.

Byakatonda, J., Parida, B.P., Kenabatho, P.K., Moalafhi, D.B., 2018b. Prediction of onset and cessation of austral summer rainfall and dry spell frequency analysis in semiarid Botswana. Theor. Appl. Climatol. 1–17. http://dx.doi.org/10.1007/s00704-017-2358-4.

Byakatonda, J., Parida, B.P., Kenabatho, P.K., Moalafhi, D.B., 2016. Modeling dryness severity using artificial neural network at the Okavango Delta, Botswana. Glob. Nest J. 18, 463–481.

Chang, F.-J., Chen, P.-A., Lu, Y.-R., Huang, E., Chang, K.-Y., 2014. Real-time multi-step-ahead water level forecasting by recurrent neural networks for urban flood control. J. Hydrol 517, 836–846. http://dx.doi.org/10.1016/j.jhydrol.2014.06.013.

Dai, A., 2013. Increasing drought under global warming in observations and models. Nat. Clim. Change 3, 52–58.

Dai, A., 2011. Characteristics and trends in various forms of the palmer drought severity index during 1900–2008. J. Geophys. Res. Atmos. 116.

De Stefano, L., Duncan, J., Dinar, S., Stahl, K., Strzepek, K.M., Wolf, A.T., 2012. Climate change and the institutional resilience of international river basins. J. Peace Res. 49, 193–209.

Dikgola, K., 2015. Spatial and Temporal Variation of Inundation in the Okavango Delta, Botswana; with Special Reference to Areas Used for Flood Recession Cultivation. University of the Western Cape.

FAO, 2001. Drought Impact Mitigation and Prevention in the Limpopo River Basin: a Situation Analysis. Rome Italy.

Feyen, L., Dankers, R., 2009. Impact of global warming on streamflow drought in Europe. J. Geophys. Res. Atmos. 114.

GOB-MEWT, 2012. Second National Communication to the United Nations Framework Convention on Climate Change (UNFCCC). Gaborone, Botswana.

GOB-MMEWR, 2006. National Water Mater Plan Review 3 Gaborone, Botswana.

Golden gate Weather Services, 2017. El Niño and La Niña Years and Intensities [WWW Document]. http://ggweather.com/enso/oni.htm (accessed 2.20.17).

Granero, M.A.S., Segovia, J.E.T., Pérez, J.G., 2008. Some comments on Hurst exponent and the long memory processes on capital markets. Phys. A Stat. Mech. its Appl. 387, 5543–5551.

Hansen, J., Sato, M., Ruedy, R., Schmidt, G.A., Lo, K., 2016. Global Temperature in 2015. Colomb. Univ., pp. 1–6.

Hayes, M., Svoboda, M., Wall, N., Widhalm, M., 2011. The Lincoln declaration on drought indices: universal meteorological drought index recommended. Bull. Am. Meteorol. Soc. 92, 485–488.

Hosking, J.R.M., Wallis, J.R., 2005. Regional Frequency Analysis: an Approach Based on L-moments. Cambridge University Press.

Huang, J., Ji, M., Xie, Y., Wang, S., He, Y., Ran, J., 2016. Global semi-arid climate change over last 60 years. Clim. Dynam. 46, 1131–1150.

Hurst, H.E., 1951. Long-term storage capacity of reservoirs. Trans. Am. Soc. Civ. Eng. 116, 770–808.

Jung, M., Reichstein, M., Ciais, P., Seneviratne, S.I., Sheffield, J., Goulden, M.L., Bonan, G., Cescatti, A., Chen, J., De Jeu, R., et al., 2010. Recent decline in the global land evapotranspiration trend due to limited moisture supply. Nature 467, 951–954.

Kenabatho, P.K., Parida, B.P., Moalafhi, D.B., 2012. The value of large-scale climate variables in climate change assessment: the case of Botswana's rainfall. Phys. Chem. Earth 50–52, 64–71. http://dx.doi.org/10.1016/j.pce.2012.08.006.

Khan, S., Gabriel, H.F., Rana, T., 2008. Standard precipitation index to track drought and assess impact of rainfall on watertables in irrigation areas. Irrigat. Drain. Syst. 22, 159–177.

Koutsoyiannis, D., 2003. Climate change, the Hurst phenomenon, and hydrological statistics. Hydrol. Sci. J. 48, 3–24.

Kundzewicz, Z.W., Kaczmarek, Z., 2000. Coping with hydrological extremes. Water Int. 25, 66–75.

Lorenzo-Lacruz, J., Vicente-Serrano, S.M., López-Moreno, J.I., Begueria, S., Garcia-Ruiz, J.M., Cuadrat, J.M., 2010. The impact of droughts and water management on various hydrological systems in the headwaters of the Tagus River (central Spain). J. Hydrol 386, 13–26.

Masih, I., Maskey, S., Mussá, F.E.F., Trambauer, P., 2014. A review of droughts on the African continent: a geospatial and long-term perspective. Hydrol. Earth Syst. Sci. 18, 3635.

Masinde, M., 2014. Artificial neural networks models for predicting effective drought index: factoring effects of rainfall variability. Mitig. Adapt. Strategies Glob. Change 19, 1139–1162. http://dx.doi.org/10.1007/s11027-013-9464-0.

Menezes, J.M.P., Barreto, G.A., 2008. Long-term time series prediction with the NARX network: an empirical evaluation. Neurocomputing 71, 3335–3343. http://dx.doi.org/10.1016/j.neucom.2008.01.030.

Mishra, A.K., Singh, V.P., 2010. A review of drought concepts. J. Hydrol 391, 202–216.

Mishra, A.K., Sivakumar, B., Singh, V.P., 2015. Drought processes, modeling, and mitigation. J. Hydrol 526, 1–2.

Moalafhi, D.B., Tsheko, R., Atlhopheng, J.R., Odirile, P.T., Masike, S., 2012. Implications of climate change on water resources of Botswana. Adv. J. Phys. Sci. 1, 4–13.

Moeletsi, M., Walker, S., 2012. Rainy season characteristics of the Free State Province of South Africa with reference to rain-fed maize production. Water SA 38, 775–782. http://dx.doi.org/10.4314/wsa.v38i5.17.

Munshi, J., 2014. There Is No Chaos in Stock Markets.

Nalbantis, I., Tsakiris, G., 2009. Assessment of hydrological drought revisited. Water Resour. Manag. 23, 881–897.

Parida, B.P., Moalafhi, D.B., 2008. Regional rainfall frequency analysis for Botswana using L-Moments and radial basis function network. Phys. Chem. Earth 33, 614–620. http://dx.doi.org/10.1016/j.pce.2008.06.011.

Pettit, A.N., 1979. Anon-parametric approach to the change-point detection. Appl. Stat 28, 126–135.

Rajasekaran, P., Prabakaran, R., Thanigaiselvan, R., 2011. Mplementation of EN-Elman backprop for dynamic power management. In: 2011 Int. Conf. Devices Commun. ICDeCom 2011-Proc, http://dx.doi.org/10.1109/ICDECOM.2011.5738531.

Richard, Y., Trzaska, S., Roucou, P., Rouault, M., 2000. Modification of the southern African rainfall variability and ENSO relationship since the late 1960s. Clim. Dynam. 16, 883–895. http://dx.doi.org/10.1007/s003820000086.

Rimkus, E., Stonevičius, E., Korneev, V., Kažys, J., Valiuškevičius, G., Pakhomau, A., 2013. Dynamics of meteorological and hydrological droughts in the Neman river basin. Environ. Res. Lett. 8, 45014.

Sakalauskiene, G., 2003. The Hurst phenomenon in hydrology. Environ. Res. Eng. Manag. 3, 16–20.

Sheffield, J., Wood, E.F., Roderick, M.L., 2012. Little change in global drought over the past 60 years. Nature 491, 435–438.

Shukla, S., Steinemann, A.C., Lettenmaier, D.P., 2011. Drought monitoring for Washington state: indicators and applications. J. Hydrometeorol. 12, 66–83.

Smakhtin, V.U., Hughes, D.A., 2004. Review, Automated Estimation and Analyses of Drought Indices in South Asia. Iwmi.

Solomon, S., 2007. Climate Change 2007-the Physical Science Basis: Working Group I Contribution to the Fourth Assessment Report of the IPCC. Cambridge University Press.

Stagge, J.H., Tallaksen, L.M., Xu, C.Y., Van Lanen, H.A.J., 2014. Standardized precipitation-evapotranspiration index (SPEI): sensitivity to potential evapotranspiration model and parameters. Proc. FRIEND-Water 367–373.

Svoboda, M., Fuchs, B., et al., 2016. Handbook of Drought Indicators and Indices.

Svoboda, M.D., Hayes, M.J., Wilhite, D.A., 2001. The role of integrated drought monitoring in drought mitigation planning. Ann. Arid Zone 40, 1–11.

Trambauer, P., Maskey, S., Werner, M., Pappenberger, F., Van Beek, L.P.H., Uhlenbrook, S., 2014. Identification and simulation of space–time variability of past hydrological drought events in the Limpopo River basin, Southern Africa. Hydrol. Earth Syst. Sci. 18, 2925–2942.

Van Loon, A.F., 2013. On the Propagation of Drought: How Climate and Catchment Characteristics Influence Hydrological Drought Development and Recovery. Wageningen University.

Van Loon, A.F., Laaha, G., 2015. Hydrological drought severity explained by climate and catchment characteristics. J. Hydrol 526, 3–14.

Vicente-Serrano, S.M., Begueria, S., López-Moreno, J.I., 2010. A multiscalar drought index sensitive to global warming: the standardized precipitation evapotranspiration index. J. Clim. 23, 1696–1718.

Vicente-Serrano, S.M., López-Moreno, J.I., 2005. Hydrological response to different time scales of climatological drought: an evaluation of the Standardized Precipitation Index in a mountainous Mediterranean basin. Hydrol. Earth Syst. Sci. Discuss. 9, 523–533.

Voss, J., 2013. Rescaled Range Analysis: a Method for Detecting Persistence, Randomness, or Mean Reversion in Financial Markets. CFA Blog.

Wada, Y., Van Beek, L.P.H., Bierkens, M.F.P., 2011. Modelling global water stress of the recent past: on the relative importance of trends in water demand and climate variability. Hydrol. Earth Syst. Sci. 15, 3785–3805.

Wilhite, D.A., 2000. Drought as a Natural Hazard: Concepts and Definitions.

Wilhite, D.A., Svoboda, M.D., Hayes, M.J., 2007. Understanding the complex impacts of drought: a key to enhancing drought mitigation and preparedness. Water Resour. Manag. 21, 763–774.

Zhang, Q., Xu, C.-Y., Zhang, Z., 2009. Observed changes of drought/wetness episodes in the Pearl River basin, China, using the standardized precipitation index and aridity index. Theor. Appl. Climatol. 98, 89–99.